

# Sgr A\*: a laboratory to measure the central black hole and stellar cluster parameters

A.A. Nucita, F. De Paolis and G. Ingrosso

*Dipartimento di Fisica, Università di Lecce, and INFN, Sezione di Lecce, CP 193, I-73100 Lecce, Italy*

A. Qadir

*Center for Advanced Mathematics and Physics, National University of Science and Technology, Campus of College of Electrical and Mechanical Engineering, Peshawar Road, Rawalpindi, Pakistan*

and

A.F. Zakharov<sup>1,2</sup>

*Institute of Theoretical and Experimental Physics, 25, B.Chermushkinskaya St., Moscow, 117259, Russia*

## ABSTRACT

Several stars orbit around a black hole candidate of mass  $3.7 \times 10^6 M_\odot$ , in the region of the Galactic Center (GC). Looking for General Relativistic (GR) periastron shifts is limited by the existence of a stellar cluster around the black hole that would modify the orbits due to classical effects that might mask the GR effect. Only if one knows the cluster parameters (its mass and core radius) it is possible to unequivocally deduce the GR effects expected and then test them. In this paper it is shown that the observation of the proper motion of Sgr A\*,  $v_{Sgr\ A^*} = (0.4 \pm 0.9) \text{ km s}^{-1}$  (Reid and Bruthaler 2004), could help us to constrain the cluster parameters significantly and that future measurements of the periastron shifts for at least three stars may adequately determine the cluster parameters and the mass of the black hole.

*Subject headings:* Gravitation — Galaxy: center — Physics of black holes

## 1. Introduction

GR predicts that orbits about a massive central body suffer periastron shifts yielding *rosette* shapes. However, the classical perturbing effects of other objects on inner orbits give an opposite shift. Since the periastron advance depends strongly on the compactness of the central body, the detection of such an effect may give information about the nature of the central body itself. This would apply for stars orbiting close to the GC, where there is a “dark object”, the black

hole hypothesis being the most natural explanation of the observational data. A cluster of stars in the vicinity of the GC (at a distance  $< 1''$ ) has been monitored by ESO and Keck teams for several years (Genzel et al. (2003 a); Schödel et al. (2003); Ghez et al. (2003, 2004, 2005)). In particular, Ghez et al. (2003) have reported on observations of several stars orbiting close to the GC massive black hole. Among those, the S2 star, with mass  $M_{S2} \simeq 15 M_\odot$ , appears to be a main sequence star orbiting the black hole with a Keplerian period of  $\simeq 15$  yrs. This yields Ghez et al. (2005) a mass estimate of  $M_{Sgr\ A^*} \simeq 3.67 \times 10^6 M_\odot$  within  $4.87 \times 10^{-3}$  pc, that is the S2 semi-major axis.

Several authors have discussed the possibility of

<sup>1</sup>Astro Space Centre of Lebedev Physics Institute, Moscow, Russia

<sup>2</sup>Bogoliubov Laboratory for Theoretical Physics, Joint Institute for Nuclear Research, Dubna, Russia

measuring the GR corrections to Newtonian orbits for Sgr A\* (see e.g. Jaroszynski 1998, 1999, 2000; Fragile & Mathews 2000; Rubilar & Eckart 2001; Weinberg, Milosavljević & Ghez 2005), usually assuming that the central body is a Schwarzschild black hole. However, since black holes generally rotate, and there is no reason why they should not be rotating fast, the Kerr metric should be used instead. Not only stellar mass black holes but also supermassive black holes are believed to be spinning. Indeed, X-ray observations of Seyfert galaxies, microquasars and binary systems (Fabian et al. (1995); Tanaka et al. (1995); Fabian et al. (2000); Fabian (2005) and references therein) show that the data could be explained by a rotating black hole model (see e.g. Zakharov & Repin (2003b,c); Zakharov et al. (2003a) and Zakharov & Repin (2004)). Further, supermassive black holes at the center of QSOs, AGNs and galaxies show beamed jet emission implying that they have non zero angular momentum. Hence, Kerr black holes may be fairly common in nature. The relatively short orbital period of the S2 star encourages a search for genuine GR effects like the orbital periastron shift. Quite possibly, more suitable stars, close to the GC black hole, will be found in the future. Bini et al. (2005) studied the GR periastron shift around Sgr A\* and estimated it for various solutions belonging to the Weyl class, including the Schwarzschild and Kerr black holes. However, they did not take into account the presence of a stellar cluster, which could in principle be sizable.

The purpose of this paper is to try to find limits for the extent and density of the cluster about Sgr A\* and if those limits yield a measurement of its spin.

Clearly, a thorough knowledge of the cluster mass and density distribution is necessary to be able to infer the mass and spin of the black hole at the GC by measuring the periastron shift and subtracting the Newtonian shift. Unfortunately, the star cluster parameters are poorly known.<sup>1</sup> However, the measure of the Brownian motion of the central black hole due to the surrounding matter may be used to constrain the black hole to

cluster mass ratio.<sup>2</sup> The latest observations of the Sgr A\* proper motion,  $v_{Sgr A^*} = (0.4 \pm 0.9) \text{ km s}^{-1}$  (Reid and Bruthaler 2004), is much tighter than the earlier one of 2–20  $\text{km s}^{-1}$  (see Reid, Readhead, Vermeulen et al. 1999).

For a test particle orbiting a Schwarzschild black hole of mass  $M_{BH}$ , the periastron shift is given by (see e.g. Weinberg, 1972)

$$\Delta\phi_S \simeq \frac{6\pi G M_{BH}}{d(1-e^2)c^2} + \frac{3(18+e^2)\pi G^2 M_{BH}^2}{2d^2(1-e^2)^2 c^4}, \quad (1)$$

$d$  and  $e$  being the semi-major axis and eccentricity of the test particle orbit, respectively. For a rotating black hole with spin parameter  $a = |\mathbf{a}| = J/GM_{BH}$ , the space-time is described by the Kerr metric and, in the most favorable case of equatorial plane motion ( $\mathbf{a} \cdot \mathbf{v} = 0$ ), the shift is given by (Boyer and Price 1965, but see also Bini et al. 2005 for more details)

$$\Delta\phi_K \simeq \Delta\phi_S + \frac{8a\pi M_{BH}^{1/2} G^{3/2}}{d^{3/2}(1-e^2)^{3/2} c^3} + \frac{3a^2\pi G^2}{d^2(1-e^2)^2 c^4}, \quad (2)$$

which reduces to eq. (1) for  $a \rightarrow 0$ . In the more general case,  $\mathbf{a} \cdot \mathbf{v} \neq 0$ , the expected periastron shift has to be evaluated numerically.

The expected periastron shifts (mas/revolution),  $\Delta\phi$  (as seen from the center) and  $\Delta\phi_E$  (as seen from Earth at the distance  $R_0 \simeq 8 \text{ kpc}$  from the GC), for the Schwarzschild and the extreme Kerr black holes, for the S2 and S16 stars turn out to be  $\Delta\phi^{S2} = 6.3329 \times 10^5$  and  $6.4410 \times 10^5$  and  $\Delta\phi_E^{S2} = 0.661$  and  $0.672$  respectively, and  $\Delta\phi^{S16} = 1.6428 \times 10^6$  and  $1.6881 \times 10^6$  and  $\Delta\phi_E^{S16} = 3.307$  and  $3.399$  respectively. Recall that

$$\Delta\phi_E = \frac{d(1+e)}{R_0} \Delta\phi_{S,K}. \quad (3)$$

Notice that the differences between the periastron shifts for the Schwarzschild and the maximally rotating Kerr black hole is at most 0.01 mas for the S2 star and 0.009 mas for the S16 star. In order to make these measurements with the required

<sup>1</sup>We remark that the star cluster we are considering around the central black hole might contain not only normal stars but also white dwarfs, neutron stars and/or stellar mass black holes.

<sup>2</sup>Other methods for estimating the black hole parameters (i.e. mass and angular momentum) based on gravitational retrolensing have been proposed. For more details on this topic we refer to De Paolis et al. (2003, 2004); Zakharov et al. (2005b); De Paolis et al. (2005); Zakharov et al. (2005a) and reference therein.

accuracy, one needs to know the S2 orbit with a precision of at least  $10 \mu\text{as}$ .

There is a proposal to improve the angular resolution of VLTI with the PRIMA facility (Röttgering et al. (2003); Delplancke et al. (2003); Quirrenbach (2003) but see also the related web-site<sup>3</sup>), which, by using a phase referenced imaging technique, will get  $\sim 10 \mu\text{as}$  angular resolution. Hence, at least in principle, the effect of a maximally rotating Kerr black hole on the periastron shift of the S2 star can be distinguished from that produced by a Schwarzschild black hole with the same mass.

The plan of the paper is as follows: In the next section we briefly discuss the effect of a central star cluster on the periastron advance. In Section 3 we use the Sgr A\* Brownian motion to constrain the black hole to star cluster mass ratio. Then we consider whether the detection of the spin of the black hole from the periastron shift of the S2 star is possible, once the cluster density and size have been adequately constrained. In Section 5 we show how future measurements of the periastron shifts for at least three stars close to the GC black hole may be used to estimate the black hole mass and the star cluster mass density distribution. In the next section we consider what the observational requirements would be for adequate determination of the cluster parameters to be able to resolve the Kerr effect. Finally, in section 7, we present some concluding remarks.

## 2. Retrograde shift due to a central stellar cluster

The star cluster surrounding the central black hole in the GC could be sizable. At least 17 members have been observed within 15 mpc up to now (Ghez et al. 2005). However, the cluster mass and density distribution, that is to say its mass and core radius, is still unknown. The presence of this cluster affects the periastron shift of stars orbiting the central black hole. The periastron advance depends strongly on the mass density profile and especially on the central density and typical length scale.

We model the stellar cluster by a Plummer

model density profile (Binney & Tremaine 1987)

$$\rho_{CL}(r) = \rho_0 f(r), \quad \text{with} \quad f(r) = \left[ 1 + \left( \frac{r}{r_c} \right)^2 \right]^{-\alpha/2}, \quad (4)$$

where the cluster central density  $\rho_0$  is given by

$$\rho_0 = \frac{M_{CL}}{\int_0^{R_{CL}} 4\pi r^2 f(r) dr}, \quad (5)$$

$R_{CL}$  and  $M_{CL}$  being the cluster radius and mass, respectively. According to dynamical observations towards the GC, we require that the total mass  $M(r) = M_{BH} + M_{CL}(r)$  contained within  $r \simeq 5 \times 10^{-3}$  pc is  $M \simeq 3.67 \times 10^6 M_\odot$ . Useful information is provided by the cluster mass fraction,  $\lambda_{CL} = M_{CL}/M$ , and its complement,  $\lambda_{BH} = 1 - \lambda_{CL}$ . As one can see, the requirement given in eq. (5) implies that  $M(r) \rightarrow M_{BH}$  for  $r \rightarrow 0$ . The total mass density profile  $\rho(r)$  is given by

$$\rho(r) = \lambda_{BH} M \delta^{(3)}(\vec{r}) + \rho_0 f(r) \quad (6)$$

and the mass contained within  $r$  is

$$M(r) = \lambda_{BH} M + \int_0^r 4\pi r'^2 \rho_0 f(r') dr'. \quad (7)$$

In Figure 1 we show the cluster mass density profile  $\rho_{CL}(r)$  as given by eq. (4), for selected values of  $\lambda_{BH}$ . The total mass  $M(r)$  enclosed within the radius  $r$  is also shown in Figure 2. In both Figures, solid, dotted and dashed lines correspond to  $\lambda_{BH} = 0, 0.7, 0.9$ , and we have assumed  $r_c = 3$  mpc (thick lines) and  $r_c = 5.8$  mpc (thin lines).

The Newtonian gravitational potential  $\Phi_N$  at a distance  $r$  due to the mass contained within it can be evaluated as

$$\Phi_N(r) = -G \int_r^\infty \frac{M(r')}{r'^2} dr'. \quad (8)$$

In Figure 3, the gravitational potential  $\Phi_N(r)$  due to the mass density distribution in eq. (6) is given for selected values of  $\lambda_{BH}$ .

According to GR, the motion of a test particle can be fully described by solving the geodesic equations. Under the assumption that the matter distribution is static and pressureless, the equation of motion of the test particle becomes (see e.g. Weinberg 1972)

$$\frac{d\mathbf{v}}{dt} \simeq -\nabla(\Phi_N + 2\Phi_N^2) + 4\mathbf{v}(\mathbf{v} \cdot \nabla)\Phi_N - v^2 \nabla\Phi_N. \quad (9)$$

<sup>3</sup><http://obswww.unige.ch/PRIMA/home/introduction>.

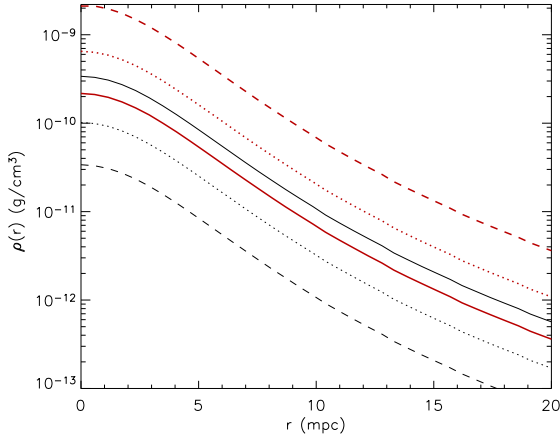


Fig. 1.— The cluster mass density profile is shown for different values of  $\lambda_{BH}$ . Solid, dotted and dashed lines correspond to  $\lambda_{BH} = 0, 0.7, 0.9$ , respectively. Thick, red lines have been obtained for  $r_c = 3$  mpc with the same values  $\lambda_{BH}$  as given above.

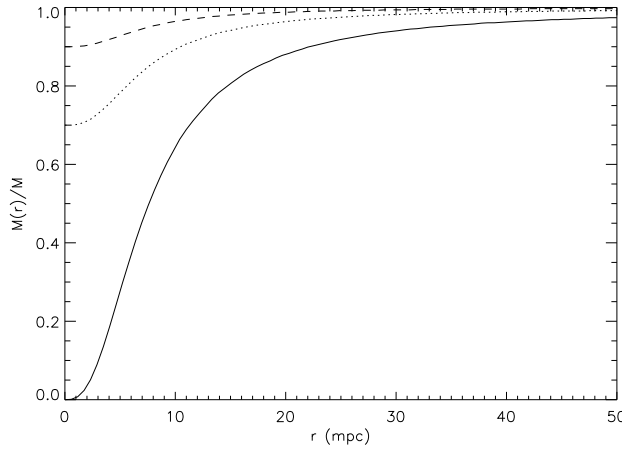


Fig. 2.— The mass enclosed within the distance  $r$  is shown for different fractions  $\lambda_{BH}$  of the total mass  $M$  which is contained in the central black hole. Solid, dotted and dashed lines correspond to  $\lambda_{BH} = 0, \lambda_{BH} = 0.7$  and  $\lambda_{BH} = 0.9$ , respectively. Note that the case corresponding to  $\lambda_{BH} = 0$  is not realistic as shown by some observations (Shen et al. (2005)).

For a spherically symmetric mass distribution<sup>4</sup> with a density profile given by eq. (4) and for a gravitational potential given by eq. (8), the previous relation becomes (see for details Rubilar et al. 2001)

$$\frac{d\mathbf{v}}{dt} \simeq -\frac{GM(r)}{r^3} \left[ \left( 1 + \frac{4\Phi_N}{c^2} + \frac{v^2}{c^2} \right) \mathbf{r} - \frac{4\mathbf{v}(\mathbf{v} \cdot \mathbf{r})}{c^2} \right], \quad (10)$$

$\mathbf{r}$  and  $\mathbf{v}$  being the radius vector of the test particle (with respect to the center of the stellar cluster) and the velocity vector, respectively. Once the initial conditions for distance and velocity are given, the orbit of a test particle can be found by solving the set of ordinary differential equations in eq. (10) numerically.

Now consider the S2 star, which is moving around the central distribution of matter on an elliptic orbit of semi-major axis  $d$  and eccentricity  $e$  in the Newtonian approximation. We take a frame with the origin in the GC,  $X$ - $Y$  plane on the orbital plane and the  $X$  axis pointing toward the periastron of the orbit. Hence, we can choose the Newtonian initial conditions to be (see e.g. Smart (1977))

$$\begin{aligned} r_x^0 &= d(1+e), \\ r_y^0 &= 0, \end{aligned} \quad (11)$$

and

$$\begin{aligned} v_x^0 &= 0, \\ v_y^0 &= \sqrt{GM(r_x^0) \left[ \frac{2}{d(1+e)} - \frac{1}{d} \right]}. \end{aligned} \quad (12)$$

For the S2 star,  $d$  and  $e$  given in the literature are 919 AU and 0.87 respectively. They yield the orbits of the S2 star for different values of the black hole mass fraction  $\lambda_{BH}$  shown in Figure 4. The Plummer model parameters are  $\alpha = 5$ , core radius  $r_c \simeq 5.8$  mpc. Note that in the case of  $\lambda_{BH} = 1$ , the expected (prograde) periastron shift is that given by eq. (1), while the presence of the stellar

<sup>4</sup>We would like to mention that the dynamical state of the region around Sgr A\* is known to be complex, with a significant population of young stars of unclear origin making the assumption of an undisturbed spherical cluster likely incorrect. Considering the effects caused by a non spherically symmetric mass distribution makes the passage to an equation similar to eq. (10) not analytically solvable. This problem will be addressed in a subsequent work.

cluster leads to a retrograde periastron shift. For comparison, the expected periastron shift for the S16 star is given in Figure 5. In the latter case, the binary system orbital parameters were taken from Schödel et al. (2003) assuming also for the S16 mass a conservative value of  $\simeq 10 M_\odot$ .

In Figure 6 the S2 orbital shift  $\Delta\Phi$  is given as a function of the stellar cluster core radius  $r_c$ , for different power law index values ( $\alpha = 4$  dashed line,  $\alpha = 5$  dotted line and  $\alpha = 6$  solid line). In the left panel, the black hole mass fraction is  $\lambda_{BH} = 0.8$  in order to compare with Rubilar et al. (2001) results, while the right panel shows the  $\lambda_{BH} = 0.99$  case. Note that for extremely compact clusters,  $\Delta\Phi$  is quite small. The same is true for large enough core radii, corresponding to matter density profiles almost constant within the S2 orbit.

Figures 4 and 6 show that the expected S2 periastron shift depends strongly on the total mass of the cluster. In particular, the shift due to the cluster is opposite in sign (retrograde motion) to the relativistic effect due to the black hole in the GC. Moreover, for each value of the cluster mass and power law index, there exist two density profiles (corresponding to two particular core radii) which have total shift almost zero, implying that the periastron advance due to the cluster is equal (in magnitude) to the periastron shift due to the black hole. A numerical analysis shows that the transition from a prograde shift (due to the black hole) to retrograde shift (due to the extended mass) occurs at  $\lambda_{BH} \simeq 0.9976, 0.9986$  and  $0.9990$  for  $\alpha = 4, 5$  and  $6$ , respectively. This means that a small fraction of mass in the cluster drastically changes the overall shift.

We would like to note that the assumption of the Plummer model to describe the mass density distribution of the stellar cluster around the central black hole is an oversimplification. Indeed, one expects that in presence of a central black hole, the stellar profile should follow a Bahcall-Wolf law with density distribution  $\rho_c(r) \propto r^{-7/4}$  (Bahcall & Wolf 1977; Binney & Tremaine 1987) at least up to  $\tilde{r}_H \ll r_H$ , where  $r_H = GM_{BH}/\sigma_*^2 \simeq 0.5$  pc is the radius of the black hole influence sphere. In the following, we call  $\tilde{r}_H$  the distance ( $\ll r_H$ ) up to which the cluster mass density follows the Bahcall-Wolf law.

In order to study the effect of such a cusp on the

expected S2 periastron shift, we consider three different cases *a)* the cusp is entirely contained within the S2 periastron distance  $R_{S2}$  (i.e.  $\tilde{r}_H \leq R_{S2}$ ), *b)* the cusp extends beyond the S2 periastron distance (thus making the S2 star move in a mass gradient) and *c)* the stellar density profile follows a cusp law up to the distance  $\tilde{r}_H$  from the center and a Plummer law for  $r \geq \tilde{r}_H$ . In cases *a)* and *b)* all stars are in a cusp density profile. In any case we require that the total mass enclosed within  $4.87 \times 10^{-3}$  pc is  $M \simeq 3.67 \times 10^6 M_\odot$ .

In case *a)*, the total S2 periastron shift is just the sum of the shift due to the black hole and the shift caused by the stellar cusp (that contributes with the same sign). Hence, the S2 shift turns out to be  $\Delta\Phi \simeq 0.17$  degree per revolution.

In case *b)*, by requiring that the total mass enclosed within  $4.87 \times 10^{-3}$  pc is  $M \simeq 3.67 \times 10^6 M_\odot$ , we find that the dependence of the cusp mass and the induced S2 periastron shift on  $\tilde{r}_H$  vanishes. Indeed, in Figure 7, we give the mass enclosed within the distance  $r$  for different values of  $\lambda_{BH}$ . Solid, dotted and dashed lines correspond to  $\lambda_{BH} = 0.1$ ,  $\lambda_{BH} = 0.5$  and  $\lambda_{BH} = 0.9$ , respectively. Figure 8 shows the expected S2 periastron shift as a function of  $\lambda_{BH}$ . As noted before, the shift due to the cluster is opposite in sign with respect to that due to the black hole. Moreover, for  $\lambda_{BH} \simeq 0.998$  the total shift turns out to be zero since the contributions of the black hole and the cluster cancel out. It is noticing that, since in the case of cusp profiles the density gradient is larger than in the case of a usual ( $\alpha = 5$ ) Plummer model, the value of the S2 periastron shift gets generally larger values. Only if the Plummer core radius is around 2 mpc the resulting S2 periastron shifts are comparable in both cases. We have then considered the superposition of a Plummer model and a Bahcall-Wolf profile (case *c)* extended up to  $\tilde{r}_H$  such as the cusp density at  $\tilde{r}_H$  equals that of the Plummer model at the same distance. Here, if  $\tilde{r}_H \ll R_{S2}$  the S2 periastron shift will be practically equal to that caused by the Plummer model (see right panel in Fig. 6) since in this case the cusp will have a minor influence. On the contrary, for an extended cusp ( $\tilde{r}_H \gg R_{S2}$ ), the cusp effect on the S2 periastron shift will dominate reconciling with case *b*.

As a last point, we mention that we have also considered the effect due to an extrapolation of the observed stellar density profile - the inner-

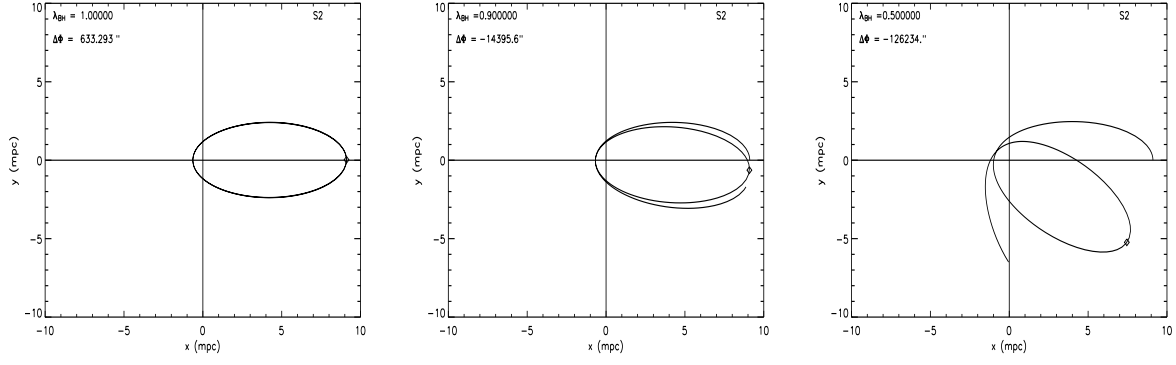


Fig. 4.— Post Newtonian orbits for different values of the black hole mass fraction  $\lambda_{BH}$  are shown for the S2 star (upper panels). Here, we have assumed that the Galactic central black hole is surrounded by a stellar cluster whose density profile follows a Plummer model with  $\alpha = 5$  and a core radius  $r_c \simeq 5.8$  mpc. The periastron shift values in each panel is given in arcseconds.

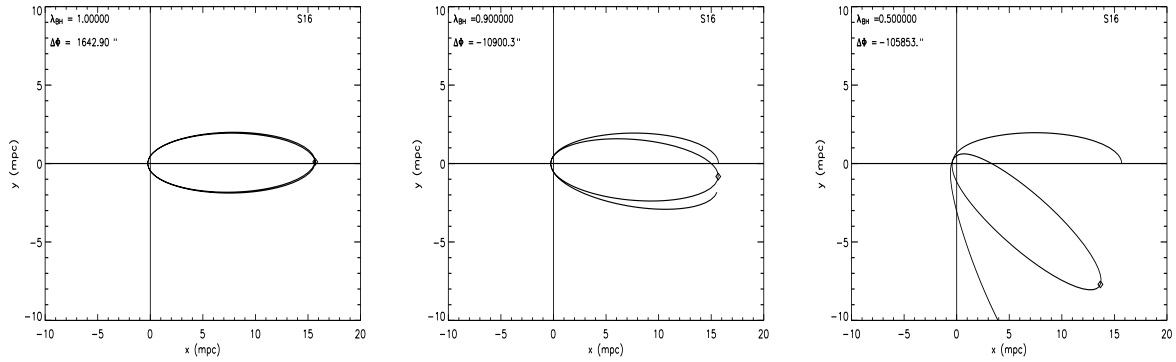


Fig. 5.— The same as in Figure 4 but for the S16–Sgr A\* binary system. In this case, the binary system orbital parameters were taken from Ghez et al. (2005) assuming for the S16 mass a conservative value of  $\simeq 10 M_\odot$ .

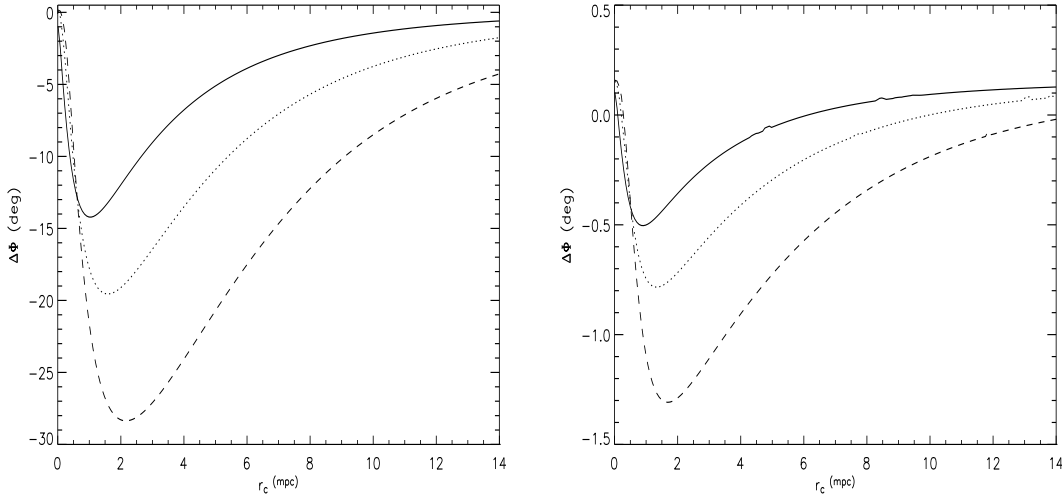


Fig. 6.— The expected S2 periastron shift as a function of the stellar cluster core radius is shown. Here we have assumed a Plummer density profile for the stellar cluster. Dashed, solid and dotted lines correspond to  $\alpha = 4, 5$  and  $6$ , respectively. The black hole mass fraction has been fixed to  $\lambda_{BH} = 0.8$  (left panel) and  $\lambda_{BH} = 0.99$  (right panel), respectively. Note the existence of a maximum approximately corresponding to the S2 semi-major axis.

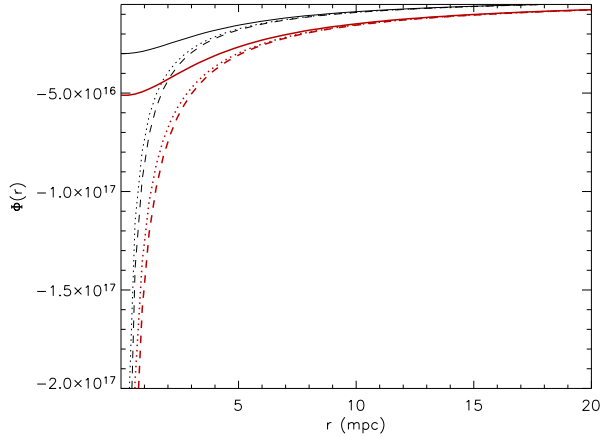


Fig. 3.— The gravitational potential at distance  $r$  as due to the mass  $M(r)$  is shown for different fractions  $\lambda_{BH}$  of the total mass  $M$ . Solid, dotted and dashed lines correspond to  $\lambda_{BH} = 0, \lambda_{BH} = 0.7$  and  $\lambda_{BH} = 0.9$ , respectively. Thick red lines have been obtained for  $r_c = 3$  mpc while thin black lines are for  $r_c = 5.8$  mpc.

most point of which is the S2 star at a distance of  $0.1''$  within  $R_{S2}$ . Following Genzel et al. (2003 b) and assuming a cusp stellar density profile, we find that the enclosed mass is in the range  $30\text{--}300 M_\odot$  (for a constant mass density or a power law with index  $\gamma = 1.4$ ). Therefore, the cusp effect on the S2 periastron shift is negligible since the corresponding  $\lambda_{BH}$  is always greater than  $0.99992$ . However, we caution that the case under investigation in the present paper is different with respect to Genzel et al. (2003 b) since we are assuming that a fraction of the mass contained within  $R_{S2}$  may be in a stellar cluster. Hence, the cluster mass content may be larger, thus providing a stronger effect on the S2 periastron shift.

### 3. Tightening mass limits of Sgr A\*

We know that the mass of Sgr A\* within the S2 orbit is  $3.67 \times 10^6 M_\odot$  to a high accuracy. Though there is nothing definite known about the mass distribution, there is strong reason to believe that there is a black hole of several solar masses, possibly surrounded by a significant cluster. In principle the cluster mass could dominate over the black

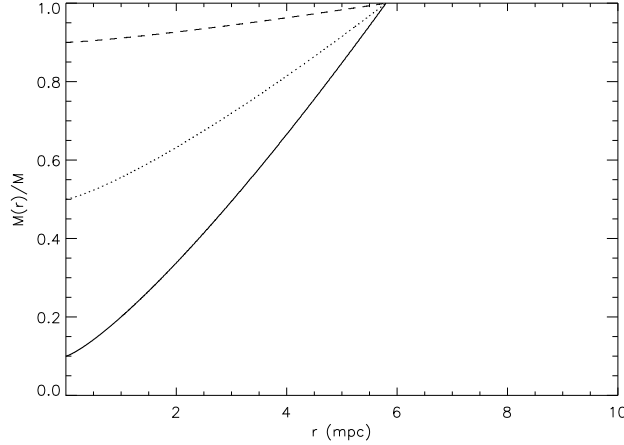


Fig. 7.— The mass enclosed within the distance  $r$  is shown for different fractions  $\lambda_{BH}$  of the total mass  $M$  contained within the S2 orbit. Solid, dotted and dashed lines correspond to  $\lambda_{BH} = 0.1$ ,  $\lambda_{BH} = 0.5$  and  $\lambda_{BH} = 0.9$ , respectively. The stellar cluster is assumed to follow an  $r^{-7/4}$  density profile.

hole, be comparable to it or be dominated by it. That there *is* a cluster is highly likely on account of the large number of stars observed near Sgr A\*. Though these lie outside the S2 orbit, many stars so far unseen probably do lie within the orbit as well. In this section we use current data on the Brownian motion of Sgr A\* and the evaporation time for the putative cluster to put limits on the cluster mass and hence on the black hole mass.

Chatterjee, Hernquist and Loeb (2002) have developed a simple model to describe the dynamics of a massive black hole surrounded by a dense stellar cluster. The total force acting on the black hole is separated into two independent parts, one of which is the slowly varying force due to the stellar ensemble and the other the rapid stochastic force due to close stellar encounters. In the case of a stellar system with a Plummer distribution, the motion of the black hole is similar to that of a Brownian particle in a harmonic potential. Thus the black hole one-dimensional mean-square velocity is given by

$$\langle v_x^2 \rangle = \frac{2}{9} \frac{GM_{CL}m_*}{r_c M_{BH}}, \quad (13)$$

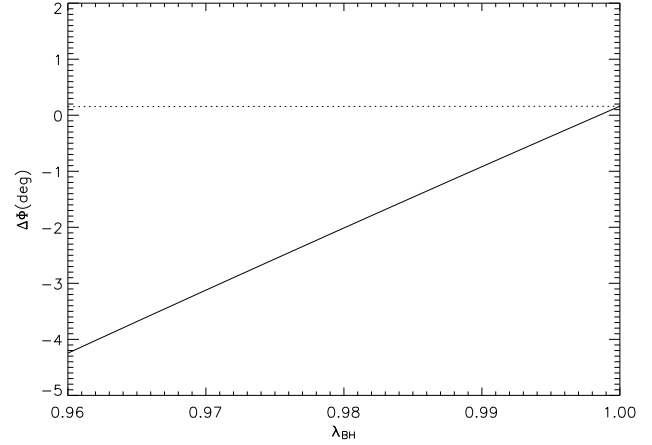


Fig. 8.— The expected S2 periastron shift as a function of the mass ratio parameter  $\lambda_{BH}$ . Solid and dashed lines correspond to the S2 shift due to the black hole and to the stellar cusp, respectively. We note that the shift due to the stellar cusp is independent on the  $\tilde{r}_H$  value, that, in this case, has been assumed to be larger than the S2 semi-major axis (case *b*).

where it has been assumed that the cluster is composed of objects with equal mass,  $m_*$ . For a Plummer ( $\alpha = 5$ ) stellar cluster, the total mass within  $R$  is

$$M(R) = M_{BH} + \frac{M_{CL}R^3}{(R^2 + r_c^2)^{3/2}}. \quad (14)$$

Since  $\langle v_x^2 \rangle$  is less than a certain maximum value  $\langle v_x^2 \rangle_{max}$ , from eqs. (13) and (14) one obtains

$$M_{BH} > M(R) \left\{ 1 + \frac{9}{2} \left[ \langle v_x^2 \rangle_{max} \frac{r_c R^3}{G(R^2 + r_c^2)^{3/2} m_*} \right] \right\}^{-1}, \quad (15)$$

the right hand side corresponding to a minimum black hole mass, as constrained by the Brownian motion of the central black hole. In Figure 9 the minimum black hole mass allowed by the Brownian motion of Sgr A\* is given as a function of the stellar cluster core radius, for two different proper motion velocities of the black hole:  $1.3 \text{ km s}^{-1}$  (dashed lines), and  $2 \text{ km s}^{-1}$  (dotted lines). The total mass contained within  $R = 0.01 \text{ pc}$  of Sgr A\* has been taken to be  $M \simeq 3.67 \times 10^6 M_\odot$ .

Chatterjee, Hernquist and Loeb (2002) derived



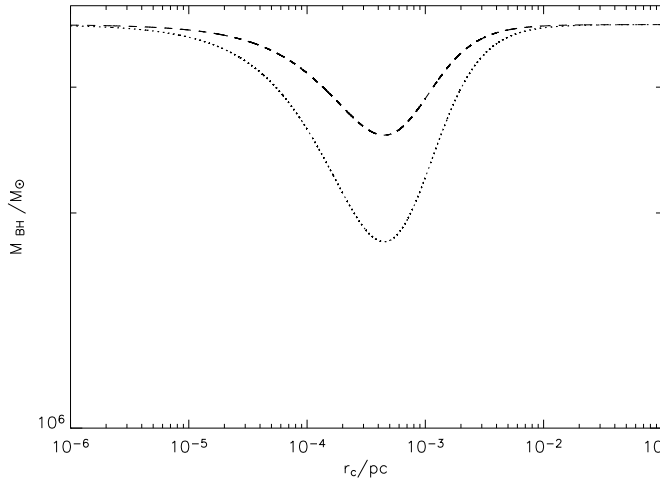


Fig. 9.— The minimum black hole mass allowed by the Brownian motion of Sgr A\* is given as a function of the stellar cluster core radius for the different black hole proper motion velocities. We assume that a total mass  $M \simeq 3.67 \times 10^6 M_\odot$  is contained within  $R_{S2} = 4.87$  mpc. Dashed and dotted lines have been obtained for velocities of  $1.3 \text{ km s}^{-1}$  and  $2 \text{ km s}^{-1}$ , respectively. For each given curve only the region above it is allowed.

an evaporation time for a cluster, but concentrated on the large scale cluster  $r_c \simeq 10$  pc about Sgr A\*, and hence assumed that  $M_{CL} \gg M_{BH}$ . On the other hand Rauch and Tremaine (1996) and Mouawad et al. (2005) consider only the region interior to the orbit of S2 and assume  $M_{CL} \ll M_{BH}$ .

We need to allow for all possibilities while considering the cluster interior to the orbit of S2, including  $M_{CL} \simeq M_{BH}$ . For this purpose we consider a cluster of core radius  $r_c$  and mass  $M_{CL} = M - M_{BH}$ . We now need to obtain the generalization of the formula of Chatterjee, Hernquist and Loeb (2002) for the median relaxation time in this more general situation. For this purpose, as usual, we assume that the cluster consists of components of the same mass  $m_*$  and evaluate the crossing time in the usual way to obtain the general median relaxation time

$$T_r = \frac{0.14(1.3 r_c M)^{3/2}}{\sqrt{G} M_{CL} m_* \log(0.4 M / m_*)}. \quad (16)$$

It is easy to verify that in the approximation  $M_{CL} \gg M_{BH}$  we recover the formula of Chatterjee, Hernquist and Loeb (2002) and in the approximation  $M_{CL} \ll M_{BH}$  we recover the formula of Rauch and Tremaine (1996). The evaporation time is then  $T_{evap} \simeq 300 T_r$  (Binney & Tremaine 1987, p.525).

One can assume different “reasonable” values of the time that the cluster would have been in existence and hence use the evaporation time to further limit the black hole mass in the GC. It is clear that  $10^8$  years = 0.1 Gyr is less than the minimum value that could be regarded as reasonable, 1 Gyr is more reasonable and 10 Gyr is likely to be a good value to take. The results are given in Table 1 for  $m_* = 1 M_\odot$ . Note that the tightest bound gives a very stringent upper limit of  $9 \times 10^4 M_\odot$  on the cluster mass. Also note that the value decreases if the average  $m_*$  is taken to be larger.

#### 4. The spin of the black hole

The periastron shift is the net contribution of the relativistic retrograde shift due to the black hole and the Newtonian prograde shift due to the surrounding cluster. Obviously, if the periastron advance due to the stellar cluster were known, the contribution of periastron advance due to the black hole could be obtained by subtracting from the measured quantity. The question arises whether the information obtained would be adequate to obtain both the black hole mass and spin parameters. Though we can put reasonably sharp bounds on the stellar cluster about the black hole, is it good enough for our purpose? If so, we could use eq.(2) to obtain the spin of the black hole for different values in the possible range for the periastron shift. It is easy to see from Fig.6 that for  $\lambda_{BH} = 0.99$  and allowing for the maximum range of unknown values of  $\alpha$  and  $r_c$  the  $1.8 \times 10^3 < -\Delta\phi < 4.7 \times 10^3$  or  $1.9 \times 10^{-3} < -\Delta\phi_E < 4.7 \times 10^{-3}$ . For the sharpest limit obtained,  $\alpha = 5$ , and Brownian motion  $1.3 \text{ km s}^{-1}$ ,  $\lambda_{BH} = 0.975$ , we find that  $\Delta\phi \simeq -4.47 \times 10^3$  or  $\Delta\phi_E \simeq -4.7 \times 10^{-3}$ . For Brownian motion  $2.0 \text{ km s}^{-1}$ ,  $\lambda_{BH} = 0.964$ ,  $\Delta\phi \simeq -5.75 \times 10^3$  or  $\Delta\phi_E \simeq -6.0 \times 10^{-3}$ . This is a factor of 5 less than the effect of the spin. Hence this method *cannot* be used to determine the spin. For this we need

| $T_{\text{evap}}(\text{Gyr})$ | $r_c^{1.3}(\text{mpc})$ | $\lambda_{\text{BH}}^{1.3}$ | $r_c^{2.0}(\text{mpc})$ | $\lambda_{\text{BH}}^{2.0}$ |
|-------------------------------|-------------------------|-----------------------------|-------------------------|-----------------------------|
| 0.1                           | 0.87                    | 0.762                       | 1.28                    | 0.645                       |
| 1                             | 2.11                    | 0.919                       | 2.61                    | 0.876                       |
| 10                            | 4.12                    | 0.975                       | 5.27                    | 0.964                       |

Table 1: The cluster core radius  $r_c$  and minimum black hole mass fraction  $\lambda_{\text{BH}}$  for the limits obtained by  $\langle v \rangle_{\text{max}}^2 = 1.3$  and 2.0, for  $T_{\text{evap}} = 0.1, 1$  and 10 Gyr.

the cluster parameter values, rather than upper limits for them. Alternatively, one would need to rely on the retrolensing method suggested earlier (De Paolis et al. 2005; ?).

## 5. Determination of cluster parameters

Using the stronger ( $1\sigma$ ) limit of  $1.3 \text{ km s}^{-1}$  and the weaker ( $2\sigma$ ) limit of  $2.0 \text{ km s}^{-1}$  to limit the Brownian motion of Sgr A\* for our calculations and evaporation times of 1 and 10 Gyr for the cluster, we obtained the minimum black hole mass. For the stronger limits on the Brownian motion and the evaporation time, it is  $3.579 \times 10^6 M_\odot$  corresponding to a  $\lambda_{\text{BH}} \simeq 0.975$  for  $\alpha = 5$ . Our numerical analysis shows that the transition from a prograde shift (due to the black hole) to a retrograde shift (due to the extended mass assumed to be distributed with a Plummer density profile) occurs at  $\lambda_{\text{BH}} \simeq 0.9976, 0.9986$  and  $0.9990$  for  $\alpha = 4, 5$  and  $6$ , respectively. Hence, even a small cluster around the central massive black hole limits the possibility to observe and use the periastron shift of the S2 star.

Since we have modeled the star cluster density profile by a Plummer model, the periastron shift contribution due to the stellar cluster depends on three parameters: the central density  $\rho_0$  (or equivalently  $\lambda_{\text{BH}}$ ); the core radius  $r_c$ ; and the power-law index  $\alpha$ . This degeneracy in the determination of the stellar cluster parameters is due to the measurement of the periastron shift of a single star. This is easily seen by inspecting Figure 10, which has been obtained for illustrative purposes for the S2 star by setting  $\lambda_{\text{BH}} = 0.99$  and varying both the core radius  $r_c$  and power-law index  $\alpha$  for the star cluster density profile. Each contour line corresponds to a given S2 periastron shift in units of degrees. To solve the parameter degeneracy and determine the stellar cluster parameters (by study-

ing the periastron advance effect), the periastron shifts for at least three different stars have to be measured with sufficient accuracy. Consider, for example, the S16 star having an orbital period of  $\simeq 36$  yr and eccentricity  $e \simeq 0.97$ . Measuring its periastron shift and comparing with the S2 result will give much tighter information about the stellar cluster parameters. From Figure 11 it is evident that there are regions (intersections between dashed and solid lines) in the  $\alpha$ - $r_c$  plane for which one measures values of the periastron shift for the S2 and S16 stars. Obviously, there could be (as yet unobserved) stars with orbit apocenters comparable to S2, but with different eccentricities (for example larger than 0.87) or stars closer to the GC black hole than S2 or S16 stars. Monitoring their orbits and measuring their periastron shifts will be extremely helpful in reconstructing the cluster density profile. As an example, in Figure 12 we compare the expected S2 periastron shift (solid lines obtained for  $\lambda_{\text{BH}} = 0.99$ ) with the periastron shift of a star whose orbit has an eccentricity of  $\simeq 0.87$  and semi-major axis 3 times smaller than that of S2.

As is evident from Figures 8 - 10, one can obtain estimates of the  $r_c$ ,  $\alpha$  and  $\lambda_{\text{BH}}$ , provided that three stars have been observed to sufficient accuracy. Assume that we have adequate accuracy of observation to see periastron shifts of  $10^{-2.5}$  mas, which is the value required to see the relativistic periastron shift. To what accuracy have we limited the cluster parameters? To determine this, we could just vary  $\lambda_{\text{BH}}$  for a given  $r_c$ . The effect of this change would be less than the effect of changing  $r_c$  and  $\lambda_{\text{BH}}$ . As such, if we want to know how accurately the cluster parameters are determined, we need to calculate the maximum change in  $r_c$  along with the change in  $\lambda_{\text{BH}}$ , as allowed by the Brownian motion limit. By varying  $\lambda_{\text{BH}}$  by  $10^{-2}$

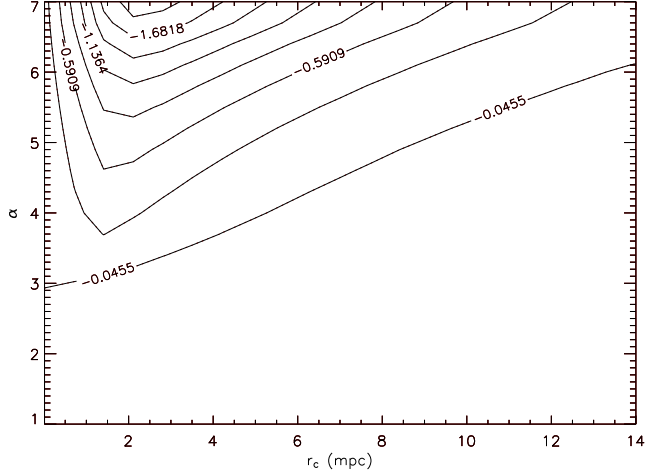


Fig. 10.— The expected S2 periastron shift for  $\lambda_{BH} = 0.99$  for different values of both the core radius  $r_c$  and power-law index  $\alpha$  for the considered Plummer density profile. Each contour line corresponds to a given S2 periastron shift in degree units. Note that a degeneracy occurs since there exist different values of the power law index and core radius corresponding to the same periastron shift.

and  $r_c$  maximally we find that we get the required accuracy, for evaporation rates from 1 to 10 Gyr and Brownian motion of 1.3 to 2.0 km s<sup>-1</sup>. With this accuracy we should also be able to separate out the classical periastron shift of the stellar cluster and the relativistic effect of a maximal (and even slightly less than maximal) Kerr black hole. With better accuracy we should be able to get an estimate, or at least an upper bound, for the black hole spin as well. The question now is, what is required to achieve this accuracy of observation of the periastron shift of three stars? This point is discussed in the next section.

## 6. Observational requirements for determination of black hole spin and cluster parameters

In the near future, observations using large diameter telescopes in combination with adaptive optics may allow us to reach the angular resolution needed to measure the periastron shift of

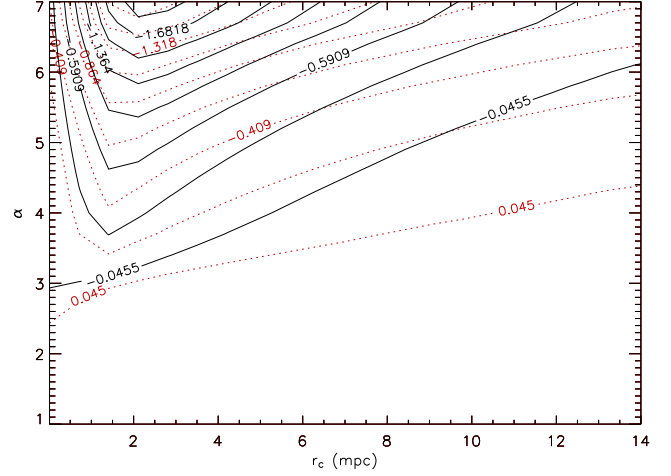


Fig. 11.— The same as in Figure 8. Dotted lines show contours for the S16 star. If the periastron shifts of both stars will be measured in the future the intersection between the corresponding contour lines will give information about the central stellar density profile.

stars close to the GC back hole. Consider for example an instrument with an angular resolution  $\Delta\Phi_A$  and assume that the relative position of stars can be determined to about  $1/\epsilon$  of the achieved angular resolution, i.e. the position accuracy is  $\Delta\Phi_P \simeq \Delta\Phi_A/\epsilon$ . The positional accuracy can be increased by a factor  $\sqrt{N}$ , if  $N$  reference stars are used. In this case, the maximum positional accuracy is simply given by (Rubilar & Eckart 2001)

$$\Delta\phi_P = \frac{\Delta\Phi_P}{\sqrt{N}}. \quad (17)$$

It follows that if the periastron position of a star shifts by an amount  $\Delta\Phi_E$  (as observed from Earth), to obtain the desired accuracy we need at least that  $\Delta\phi_P \simeq \Delta\Phi_E$ . In this case, the minimum number of reference stars can be determined once both the instrument angular and positional accuracies are known, i.e.

$$N_{max} = \left( \frac{\Delta\Phi_P}{\Delta\Phi_E} \right)^2. \quad (18)$$

As an example, the LBT interferometer has angular resolution  $\Delta\Phi_A \simeq 30$  mas and the rela-

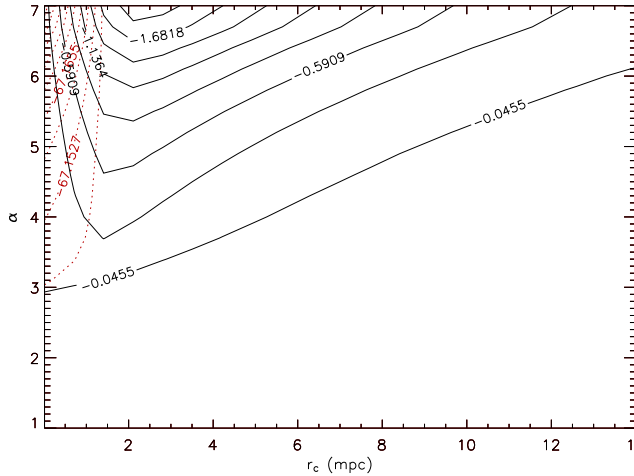


Fig. 12.— The same as in Figure 8. Dotted lines show contours for a star with orbit of  $\simeq 0.87$  (the same as the S2 star) but semi-major axis 3 times smaller with respect to the S2 one. If the periastron shifts of both stars will be observed in the future the intersection between the corresponding contour lines gives information about the central stellar density profile.

tive position of stars is conservatively estimated to be about  $1/30$  of that value (Rubilar & Eckart 2001). Therefore, to measure the periastron shift with adequate accuracy to see the least shift for the cluster parameters allowed, and thereby detect the relativistic shift, we need  $N$  to be  $\simeq (6.6 \times 10^{-1}/2 \times 10^{-3})^2$  or  $10^5$  reference stars, which automatically provides the accuracy required to see the maximal Kerr (spin) effect. For PRIMA (see <http://www.eso.org/projects/vlti/instru/prima/index.prima.html>) the relative positional accuracy is planned to be  $\simeq 10 \mu\text{as}$ . As such, we only need a single reference star.

## 7. Concluding remarks

We have used the fact that the stellar cluster close to the central black hole seems spherically symmetric to limit the Brownian motion of Sgr A\* to be the observed proper motion. We have taken the stronger ( $1\sigma$ ) limit of  $1.3 \text{ km s}^{-1}$  and the weaker ( $2\sigma$ ) limit of  $2.0 \text{ km s}^{-1}$  for our calculations. We also used evaporation times of 1

to 10 Gyr for the cluster, appropriately modified to incorporate the gravitational well due to the black hole, to put further constraints on the cluster mass. The results of our calculations show that the stellar periastron shifts due to the cluster, even limited to the extent considered, may totally swamp not only the Kerr (spin) effect but also the Schwarzschild effect. However, the discussion focused on the observations for a single star, S2. By modelling the star cluster density profile with a Plummer low, the periastron shift contribution due to the stellar cluster depends on three parameters: the central density  $\rho_0$  (or equivalently  $\lambda_{BH}$ ), the core radius  $r_c$ , and the power-law index  $\alpha$ . Consequently, with observations of three stars we should be able to determine the cluster parameters adequately.<sup>5</sup> We have addressed the question of what is required to obtain the desired accuracy for observing the relativistic effect. It turns out that we need about  $10^5$  reference stars with the LBT interferometer. With the accuracy expected of PRIMA, it should be enough to use only one reference star.

This work has been partially supported by MIUR (Programmi di Ricerca Scientifica di Rilevante Interesse Nazionale (PRIN04) - prot. 2004020323\_004). We would like to thank an unknown referee for very useful suggestions and comments that have improved our paper. Two of us (AQ and AFZ) would like to thank the Department of Physics of University of Lecce and INFN (Italy) where this work has been initiated. FDP and AAN would like to thank the 30<sup>th</sup> International Nathiagali Summer College (Pakistan), where the original version of this work has been completed. AFZ is also grateful to the National Natural Science Foundation of China (NNSFC) (Grant # 10233050) and National Key Basic Research Foundation (Grant # TG 2000078404) for a partial financial support of the work.

## REFERENCES

- Bachall J.N. and Wolf R.A. 1977, ApJ, 216, 883  
 Bini D. et al. 2005, Gen. Rel. Grav., 37, 1263

<sup>5</sup>Note that, whether we would have known that the star cluster follows a Bahcall-Wolf profile, by measuring the periastron advance of only one star we may be able to calculate the only parameter:  $\lambda_{BH}$  (from Fig. 8).

- Binney J. and Tremaine S., *Galactic Dynamics*, Princeton University Press, Princeton, New Jersey, 1987
- Boyer R.H. and Price T.G. 1965, Proc. Camb. Phil. Soc. 61, 531
- Chatterjee P., Hernquist L. and Loeb A. 2002, ApJ, 572, 371
- Delplancke F. et al. 2003, A&A, 286, 99
- De Paolis F. et al. 2003, A&A, 409, 809
- De Paolis F. et al. 2004, A&A, 415, 1
- De Paolis F. et al. 2005, in *Proc. Eleventh Regional Conf. on Math. Phys.* eds. Rahvar S, Sadooghi N, and Shojai F, World Scientific
- Fabian A.C. 2005, Ap&SS, 300, 97
- Fabian A.C. et al. 2000, PASP, 112, 1145
- Fabian A.C. et al. 1995, MNRAS, 277, L11
- Fragile P.C. & Mathews G.J. 2000, ApJ, 542, 328
- Genzel R. et al. 2003 a, Nature, 425, 934
- Genzel R. et al. 2003 b, ApJ, 594, 812
- Ghez A.M. et al. 2003, ApJ, 586, L127
- Ghez A.M., et al. 2004, ApJ, 601, L159
- Ghez A.M., et al. 2005, ApJ, 620, 744
- Jaroszynski M. 1998, Acta Astron., 48, 653
- Jaroszynski M. 1999, ApJ, 521, 591
- Jaroszynski M. 2000, Acta Astron., 50, 67
- Mouawad N. et al. 2005, Astron. Nachr., 326, 83
- Quirrenbach A. 2003, Ap& SS, 286, 277
- Rauch K.P. & Tremaine S. 1996, NewA 1, 149
- Reid M.J. and Brunthaler A. 2004, ApJ, 616, 872
- Reid M.J. et al. 1999, ApJ, 524, 816
- Röttgering H.J.A. et al. 2003, astro-ph/0308538
- Rubilar G.F. & Eckart A. 2001, A&A, 374, 95
- Schödel R. et al. 2003, ApJ, 596, 1015
- Shen Z.-Q. et al. 2005, Nature, 438, 62
- Smart W.M. 1977, *Textbook on Spherical Astronomy*, Cambridge University Press
- Tanaka Y. et al. 1995, Nature, 375, 659
- Weinberg N.N., Milosavljević M. & Ghez A.M. 2005, ApJ, 622, 878
- Weinberg S. 1972, *Gravitation and Cosmology: Principles and Applications of the General Theory of Relativity*, Wiley, New York
- Zakharov A.F. et al. 2003a, MNRAS, 342, 1325
- Zakharov A.F. et al. 2005a, New Astronomy, 10, 479
- Zakharov A.F. et al. 2005b, A&A, 442, 795
- Zakharov A.F. & Repin S.V. 2003b, A&A, 406, 7
- Zakharov A.F. & Repin S.V. 2003c, Astron. Rep., 47, 733
- Zakharov A.F. & Repin S.V. 2004, Adv. Space Res., 34, 1837